Detached Eddy Simulation coupled with steady RANS in the wall region

Lars Davidson

Division of Fluid Dynamics
Dept. of Mechanics and Maritime Sciences
SE-412 96 Gothenburg, Sweden

November 26, 2021

DES — Detached-Eddy Simulations

- Problem:

DES — Detached-Eddy Simulations

- Problem:
  - the flow in the RANS region is highly unsteady (i.e. URANS)

DES — Detached-Eddy Simulations

- Problem:
  - the flow in the RANS region is highly unsteady (i.e. URANS)
  - this means that RANS turbulence models (developed for steady flow) are not accurate

DES — Detached-Eddy Simulations

- Problem:
  - the flow in the RANS region is highly unsteady (i.e. URANS)
  - this means that RANS turbulence models (developed for steady flow) are not accurate
- Solution:

DES — Detached-Eddy Simulations

- Problem:
  - the flow in the RANS region is highly unsteady (i.e. URANS)
  - this means that RANS turbulence models (developed for steady flow) are not accurate
- Solution:
  - solve the steady equations in the RANS region

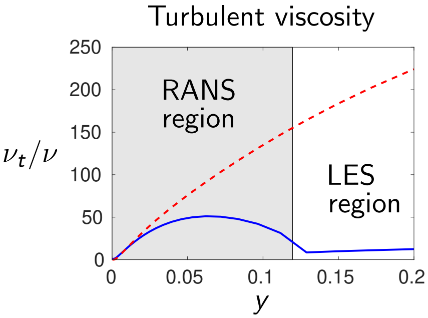

Figure: Channel flow. ——— : DES; – – ; 1D steady RANS.

Two solvers

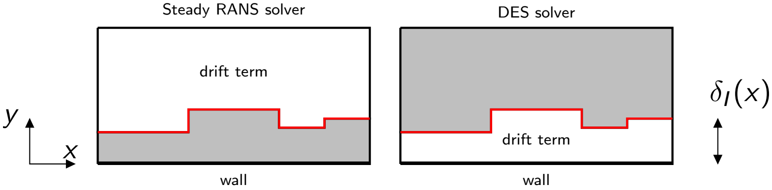

Figure: Grey color indicates the solver that drives the flow

Two solvers

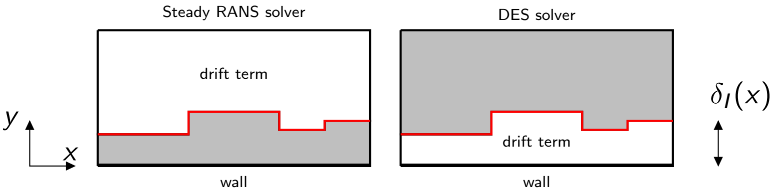

Figure: Grey color indicates the solver that drives the flow

- The interface, $\delta_I(x)$, is defined by the usual DES switch

$$F_{DES} = \max\left\{\frac{L_t}{\Delta}, 1\right\} = \max\left\{\frac{k^{1/2}/(C_\mu\omega)}{\Delta}, 1\right\}$$

Momentum Equations

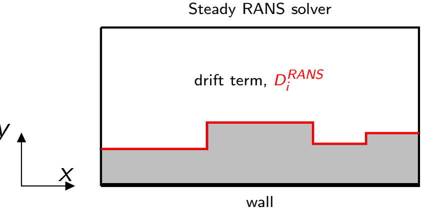

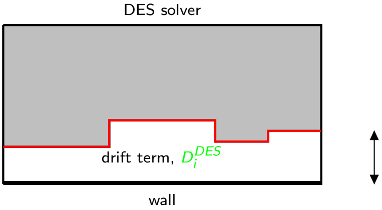

$$\frac{\partial \langle \bar{v}_j \rangle \langle \bar{v}_i \rangle}{\partial x_j} = S_i^{RANS} - \frac{1}{\rho}\frac{\partial \langle \bar{p} \rangle}{\partial x_i} + \frac{\partial}{\partial x_j}\left((\nu + \langle \nu_t \rangle) \frac{\partial \langle \bar{v}_i \rangle}{\partial x_j} \right)$$

$$\langle \bar{v}_i \rangle^{RANS} \Rightarrow \langle \bar{v}_i \rangle_T^{DES}$$

$$S_i^{RANS} = \frac{\langle v_i^{DES} \rangle_T - \langle v_i^{RANS} \rangle}{10^{-10}}$$

$$\frac{\partial \bar{v}_i}{\partial t} + \frac{\partial \bar{v}_j \bar{v}_i}{\partial x_j} = S_i^{DES} - \frac{1}{\rho}\frac{\partial \bar{p}}{\partial x_i} + \frac{\partial}{\partial x_j}\left((\nu + \nu_t) \frac{\partial \bar{v}_i}{\partial x_j} \right)$$

$$\langle \bar{v}_i \rangle_T^{DES} \Rightarrow \langle \bar{v}_i \rangle^{RANS}$$

$$S_i^{DES} = \frac{\langle v_i^{RANS} \rangle - \langle \bar{v}_i^{DES} \rangle_T}{\tau_r}$$

Time Averaging

- Subscript T indicates averaging time (memory $= T$)

$$\langle \phi(t) \rangle_T = \frac{1}{T} \int_{-\infty}^{t} \phi(\tau) \exp(-(t-\tau)/T) d\tau \Rightarrow$$

$$\langle \phi \rangle_T^t \equiv \langle \phi \rangle_T = a \langle \phi \rangle_T^{t-\Delta t} + (1-a)\phi^t$$

$$a = \exp(-\Delta t / T).$$

$$\tau_r = \max(0.1k/\varepsilon, \Delta t)$$

Numerical Method: Finite Volume Methods

- CALC-BFC [6]
- 2D RANS solver
- Staggered grid
- SIMPLEC
- $\bar{u}$, $\bar{v}$, $\bar{w}$: 2nd order upwind
- k & ω: Hybrid 1^{st} order
- Steady

- CALC-LES [5]
- 3D DES solver
- Collocated grid
- Pressure-velocity: fractional step
- $\bar{u}$, $\bar{v}$, $\bar{w}$: Central differences (CDS)
- k & ω: Hybrid 1^{st} order upwind/C
- Crank-Nicholson in time

Turbulence Models

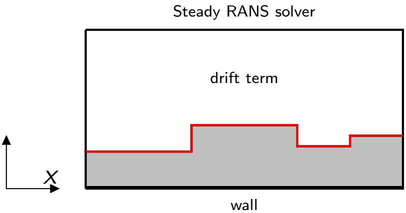

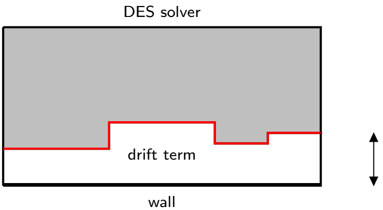

- EARSM (Explicit Algebraic Stress Model) [9]
- coupled to Wilcox $k - \omega$ model [10]

- DES $k - \omega$ model

Coupling in the RANS Solver

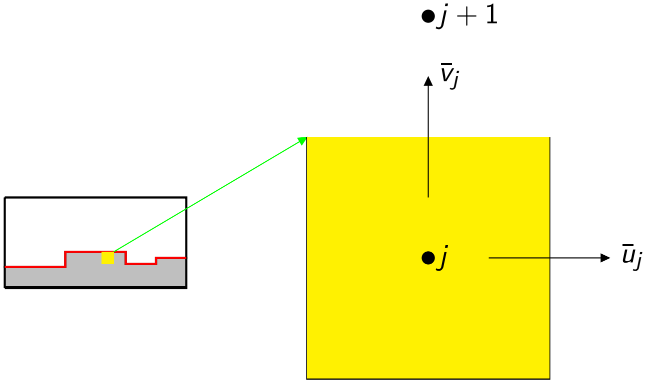

Figure: Cell j in RANS solver adjacent to the interface.

- $\langle \bar{p}_{j+1}^{LES} \rangle_T$, $\langle \bar{u}_{j+1}^{LES} \rangle_T$, at the LES-RANS interface are used as a boundary condition for the RANS solver in the wall region
- The wall-normal velocity, $\bar{v}_j^{RANS}$, is solved for using the pressure at node $j+1$.

First Test Case: Channel flow

- We denote the method NZ S-DES (Non-Zonal approach using Steady RANS coupled to DES)

First Test Case: Channel flow

- We denote the method NZ S-DES (Non-Zonal approach using Steady RANS coupled to DES)
- Reynolds number is $Re_\tau = 8\,000$.
- A $32 \times 96 \times 32$ mesh is used
- $x_{max} = 3.2$, $z_{max} = 1.6$, 15% stretching in y direction

Channel flow: Velocity

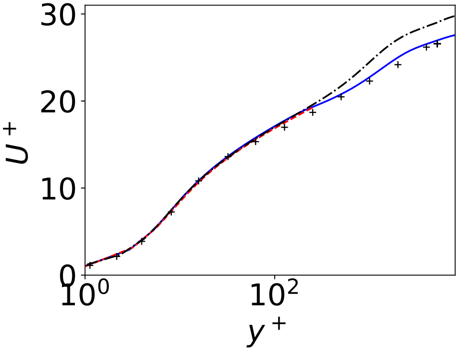

Figure: Channel flow. NZ S-DES compared with standard *DES*. (blue solid line): DES solver in NZ S-DES; (red dashed line): RANS solver in NZ S-DES; (black dash-dot line): Standard DES; +: Reichardt's law,

$U^+ = \frac{1}{\kappa}\ln(1 - 0.4y^+) + 7.8\,[1 - \exp(-y^+/11) - (y^+/11)\exp(-y^+/3)]$.

Channel flow: Shear Stresses

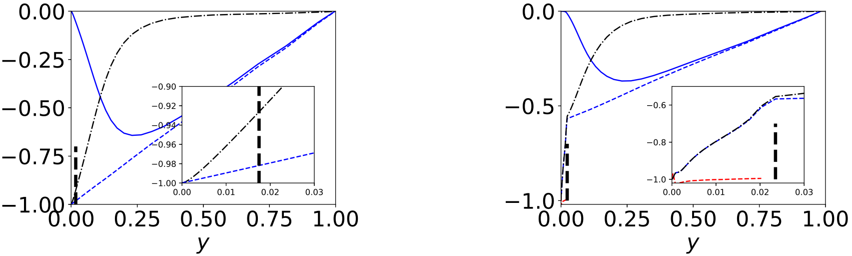

(A) Standard DES. (B) NZ S-DES .

Figure: Vertical black dashed lines show RANS-LES interface. : resolved; : viscous + modeled; : total. : viscous plus modeled in RANS solver (EARSM) in NZ S-DES .

Channel flow: Forces

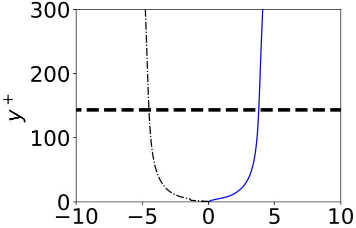

(A) Standard DES.

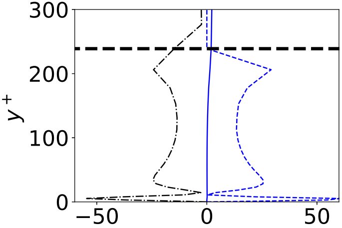

(B) NZ S-DES .

Figure: Forces in the $\langle \bar{u}_1 \rangle$ equation. ——— : $-\dfrac{\partial \langle u'v' \rangle}{\partial x_2}$; — · — : $\dfrac{\partial}{\partial x_2}\left(\langle \nu_{tot} \rangle \dfrac{\partial \langle \bar{u} \rangle}{\partial x_2} \right)$; - - : Drift term, S_1^{DES}.

Shear Stresses Including Drift Term

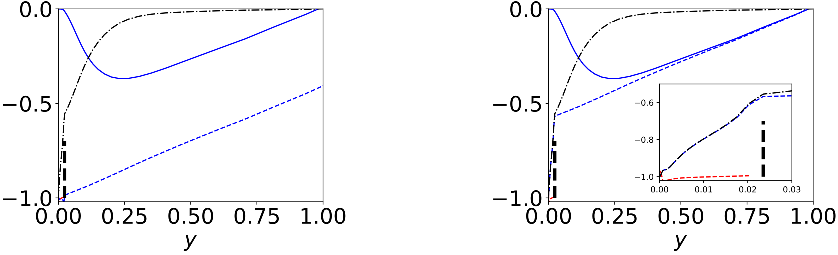

(A) NZ S-DES. ▬ ▬ : total, including $D(y) = \int_0^y S_1^{DES}(\eta)d\eta$.

(B) NZ S-DES.

Figure: Vertical black dashed lines show RANS-LES interface. ▬▬ : resolved; ▬ · ▬ : viscous + modeled; ▬ ▬ : total. ▬ ▬ : viscous plus modeled in RANS solver (EARSM) in NZ S-DES.

Flat-Plate Boundary Layer

- $Re_\theta = 6100$.
- Mesh: $1024 \times 160 \times 64$ cells (x, y, z)
- $\Delta z^+_{in} = 85$ and $\Delta x^+_{in} = 280$.
- Anisotropic, synthetic turbulence at inlet [3, 1].
- Commutation terms in the k and ω equations are used at inlet [4, 1].

Skin Friction and Velocities

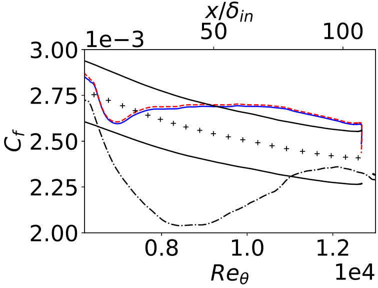

(A) Skinfriction v. momentum thickness. $+$: expts; ▬▬ : $\pm 6\%$

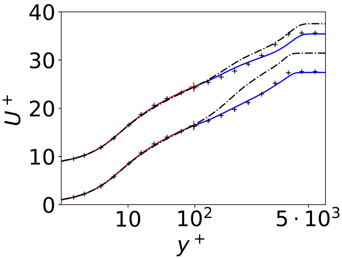

(B) Mean velocity. Lower lines: x/δ_{in} $Re_\theta = 8\,000$; upper lines: $x/\delta_{in} =$ $Re_\theta = 10\,500$. $+$ DNS at $Re_\theta = 8$

Figure: ▬▬ : NZ S-DES ; ▬ · ▬ : Standard DES; ▬ ▬ : RANS solver in NZ S-DES .

Shear Stresses

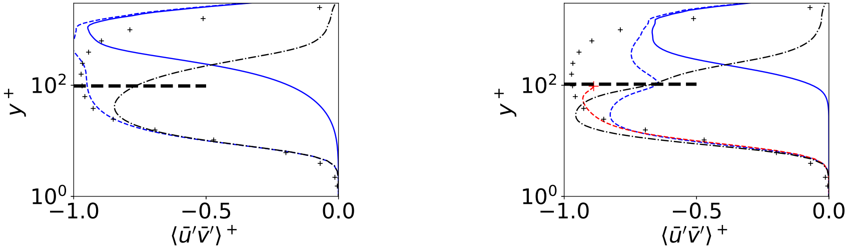

(A) Standard DES (B) NZ S-DES .

Figure: $x/\delta_{in} = 75, Re_\theta = 10\,200$. blue solid line : resolved; black dash-dot line : viscous plus modeled; blue dashed line : total; red dashed line : viscous plus modeled in RANS solver (EARSM) in NZ S-DES ; + DNS at $Re_\theta = 8\,000$

Third Test Case: Hump flow

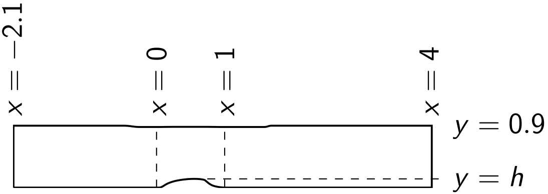

Figure: The domain of the hump. $z_{max} = 0.3$.

- The Reynolds number of the hump flow is $Re_c = 936\,000$.
- The mesh has $648 \times 108 \times 64$ cells (x, y, z) with $\Delta t = 0.0015$
- Grid from NASA workshop[1]; refined near the inlet and outlet.
- Inlet is located at $x = -2.1$ and the outlet at $x = 4.0$,
- Experiments by [8, 7]

[1] https://turbmodels.larc.nasa.gov/nasahump_val.html

Pressure and Skin Friction

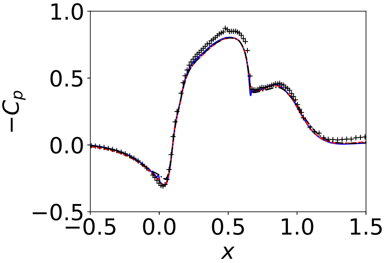

(A) Pressure ▬▬ : ±6%

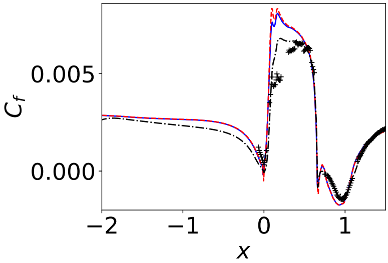

(B) Skin friction.

Figure: Pressure and skin friction. ▬▬ : NZ S-DES ; ▬ · ▬ : Standard DES; ‒ ‒ : RANS solver in NZ S-DES . +: expts. [8, 7]

Velocities

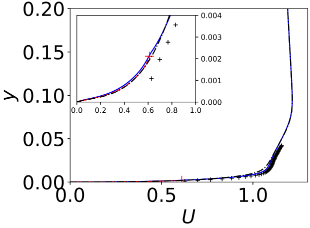

(A) $x = 0.65$

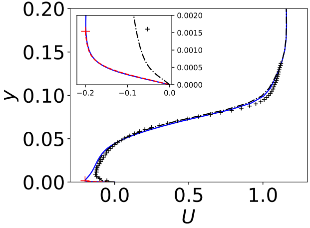

(B) $x = 0.80$

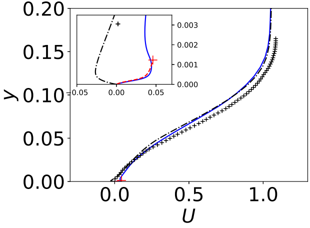

(C) $x = 1.1$

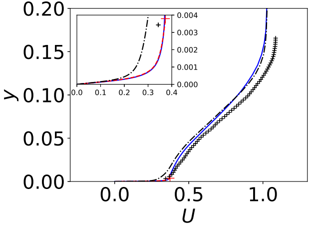

(D) $x = 1.3$

Figure: ▬ : NZ S-DES ; ▬ · ▬ : Standard DES; ▬ ▬ : RANS solver

Shear Stresses

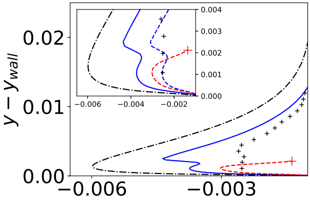

(A) $x = 0.65$

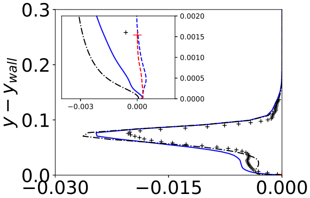

(B) $x = 0.80$

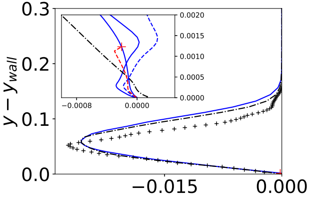

(C) $x = 1.1$

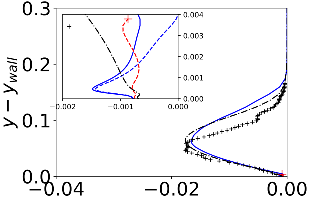

(D) $x = 1.3$

Figure: —— : NZ S-DES ; — · — : Standard DES; - - - : RANS solver

Forces

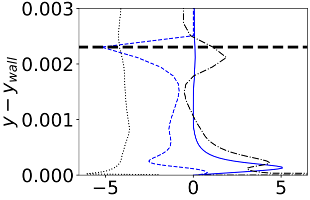

(A) $x = 0.65$

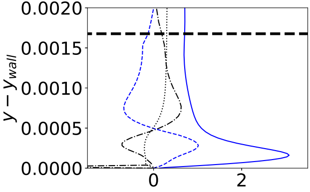

(B) $x = 0.80$

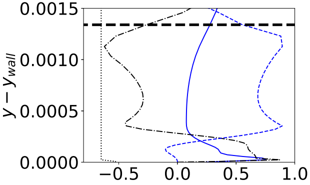

(C) $x = 1.1$

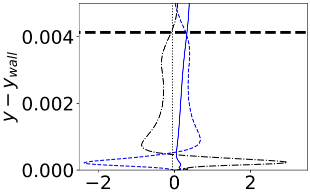

(D) $x = 1.3$

Figure: (solid blue line) : $-\dfrac{\partial\langle u'v'\rangle}{\partial y}$; (dash-dot black line) : $\dfrac{\partial}{\partial y}\left(\langle\nu_{tot}\rangle\dfrac{\partial\langle\bar{u}\rangle}{\partial y}\right)$; (dotted black line) : $-\dfrac{\partial\langle p\rangle}{\partial x}$; (dashed blue line) : Drift term, S_1^{DES}.

Conclusions

- A new steady RANS coupled to DES (N-Z S-DES) is proposed.

Conclusions

- A new steady RANS coupled to DES (N-Z S-DES) is proposed.
- Very good results for channel flow and flat-plate boundary layer (much better than standard DES)

Conclusions

- A new steady RANS coupled to DES (N-Z S-DES) is proposed.
- Very good results for channel flow and flat-plate boundary layer (much better than standard DES)
- Hump flow: similar results as standard DES

Conclusions

- A new steady RANS coupled to DES (N-Z S-DES) is proposed.
- Very good results for channel flow and flat-plate boundary layer (much better than standard DES)
- Hump flow: similar results as standard DES
- The new model is very robust regarding location of RANS-LES interface, $50 < y^+ < 200$ (not shown here)

Conclusions

- A new steady RANS coupled to DES (N-Z S-DES) is proposed.
- Very good results for channel flow and flat-plate boundary layer (much better than standard DES)
- Hump flow: similar results as standard DES
- The new model is very robust regarding location of RANS-LES interface, $50 < y^+ < 200$ (not shown here)
- EARSM is used in the RANS solver: it is found that $k - \omega$ performs equally well (not shown here)

Conclusions

- A new steady RANS coupled to DES (N-Z S-DES) is proposed.
- Very good results for channel flow and flat-plate boundary layer (much better than standard DES)
- Hump flow: similar results as standard DES
- The new model is very robust regarding location of RANS-LES interface, $50 < y^+ < 200$ (not shown here)
- EARSM is used in the RANS solver: it is found that $k - \omega$ performs equally well (not shown here)
- The 2D RANS solver increase the CPU by 10%

Conclusions

- A new steady RANS coupled to DES (N-Z S-DES) is proposed.
- Very good results for channel flow and flat-plate boundary layer (much better than standard DES)
- Hump flow: similar results as standard DES
- The new model is very robust regarding location of RANS-LES interface, $50 < y^+ < 200$ (not shown here)
- EARSM is used in the RANS solver: it is found that $k - \omega$ performs equally well (not shown here)
- The 2D RANS solver increase the CPU by 10%
- Future development: replace full RANS solver with boundary-layer solver prescribing the pressure gradient from the DES solver [2]

References I

[1] S. Arvidson, L. Davidson, and S.-H. Peng. Interface methods for grey-area mitigation in turbulence-resolving hybrid RANS-LES. *International Journal of Heat and Fluid Flow*, 73:236–257, 2018.

[2] J.-A. Bäckar and L. Davidson. Evaluation of numerical wall functions on the axisymmetric impinging jet using OpenFOAM. *International Journal of Heat and Fluid Flow*, 67:27–42, 2017.

[3] L. Davidson. Zonal PANS: evaluation of different treatments of the RANS-LES interface. *Journal of Turbulence*, 17(3):274–307, 2016.

[4] L. Davidson. Two-equation hybrid RANS-LES models: A novel way to treat k and ω at inlets and at embedded interfaces. *Journal of Turbulence*, 18(4):291–315, 2017.

References II

[5] L. Davidson. CALC-LES: a Fortran code for LES and hybrid LES-RANS. Technical report, Division of Fluid Dynamics, Dept. of Mechanics and Maritime Sciences, Chalmers University of Technology, Gothenburg, 2018.

[6] L. Davidson and B. Farhanieh. CALC-BFC: A finite-volume code employing collocated variable arrangement and cartesian velocity components for computation of fluid flow and heat transfer in complex three-dimensional geometries. Rept. 95/11, Dept. of Thermo and Fluid Dynamics, Chalmers University of Technology, Gothenburg, 1995.

[7] D. Greenblatt, K. B. Paschal, C.-S. Yao, and J. Harris. A separation control CFD validation test case Part 1: Zero efflux oscillatory blowing. AIAA-2005-0485, 2005.

References III

[8] D. Greenblatt, K. B. Paschal, C.-S. Yao, J. Harris, N. W. Schaeffler, and A. E. Washburn. A separation control CFD validation test case. Part 1: Baseline & steady suction. AIAA-2004-2220, 2004.

[9] S. Wallin and A. V. Johansson. A new explicit algebraic Reynolds stress model for incompressible and compressible turbulent flows. *Journal of Fluid Mechanics*, 403:89–132, 2000.

[10] D. C. Wilcox. Reassessment of the scale-determining equation. *AIAA Journal*, 26(11):1299–1310, 1988.